



OPEN ACCESS

EDITED BY

Xiaofei Tan,
Hunan University, China

REVIEWED BY

Marco Carnevale Miino,
University of Insubria, Italy
Selvankumar Thangaswamy,
Saveetha University, India

*CORRESPONDENCE

Muzammil Anjum,
✉ muzammilanjum@gmail.com
Zepeng Rao,
✉ raozepeng@zju.edu.cn
Habib Ullah,
✉ habib901@zju.edu.cn

†These authors have contributed equally to this work

RECEIVED 18 December 2024

ACCEPTED 19 March 2025

PUBLISHED 09 April 2025

CITATION

Lian F, Batool F, Anjum M, Qadeer S, Idris AM, Nisa W-u, Rao Z and Ullah H (2025)

Transforming apricot kernel shell into a multifunctional photocatalyst for wastewater treatment and antimicrobial applications.

Front. Environ. Sci. 13:1547291.

doi: 10.3389/fenvs.2025.1547291

COPYRIGHT

© 2025 Lian, Batool, Anjum, Qadeer, Idris, Nisa, Rao and Ullah. This is an open-access article distributed under the terms of the [Creative Commons Attribution License \(CC BY\)](https://creativecommons.org/licenses/by/4.0/). The use, distribution or reproduction in other forums is permitted, provided the original author(s) and the copyright owner(s) are credited and that the original publication in this journal is cited, in accordance with accepted academic practice. No use, distribution or reproduction is permitted which does not comply with these terms.

Transforming apricot kernel shell into a multifunctional photocatalyst for wastewater treatment and antimicrobial applications

Faqin Lian^{1†}, Fareena Batool^{2†}, Muzammil Anjum^{2*}, Samia Qadeer³, Abubakr M. Idris⁴, Waqar-un-Nisa⁵, Zepeng Rao^{6,7*} and Habib Ullah^{6*}

¹School of environmental science and engineering, Hainan University, Haikou, China, ²Department of Environmental Sciences, Institute of Soil and Environmental Sciences, PMAS Arid Agriculture University, Rawalpindi, Pakistan, ³Department of Environmental Sciences, Allama Iqbal Open University, Islamabad, Pakistan, ⁴Department of Chemistry, College of Science, King Khalid University, Abha, Saudi Arabia, ⁵Center for Interdisciplinary Research in Basic Sciences, International Islamic University, Islamabad, Pakistan, ⁶Innovation Center of Yangtze River Delta, Zhejiang University, Zhejiang, China, ⁷Department of Environmental Science, Zhejiang University, Zhejiang, China

Introduction: Industrial wastewater (WW) has emerged as one of the significant environmental problems posing serious concerns to aquatic and human health. Among various industries, pharmaceutical compounds have been detected in various aquatic environments and food supply chains; therefore, they need an economical and efficient treatment process. Photocatalysis is a promising technology for addressing environmental pollution, such as wastewater treatment and microbial disinfection.

Methods: In this study, a novel visible light-active photocatalyst was developed using activated carbon (AC) derived from local biomass; apricot kernel shell (AKS) and modified with Ag₂O/ZnO. The synthesized photocatalyst (AC/Ag₂O/ZnO) was characterized by using various tools such as XRD, UV-Visible spectroscopy and FTIR. Extensive experiments were performed to test AC/Ag₂O/ZnO for its multi-application potential, such as degradation of selected organic pollutants, treatment of pharmaceutical WW and heavy metal removal, and microbial disinfection. In the first set of experiments, the reactive black azo dye was used as the selected model pollutant and optimized for various operating conditions such as time, pH, pollutant concentration, and catalyst dose. In the second phase, pharmaceutical WW was treated using a photocatalysis process compared to photolysis (without catalyst). The third experimental setup, AC/Ag₂O/ZnO was evaluated for its disinfection potential against common pathogens, including *Escherichia coli*, *Staphylococcus aureus*, and *Pseudomonas aeruginosa*.

Results and Discussion: The results demonstrated up to 99% removal of reactive black azo dye within 4 h under optimum operation conditions, i.e., pH of 5.0, pollutant concentration of 10 ppm, and a catalyst dosage of 0.5 g/L. In the case of pharmaceutical WW, a significant reduction in chemical oxygen demand (COD) from 1195 to 199 mg/L was achieved, outperforming photolytic treatment, which reduced 1283.5 mg/L to 956 mg/L. The antimicrobial activity test showed efficient

bacterial inhibition, with the zone of inhibition (ZOI) measuring 7 mm for *E. coli*, 12 mm for *S. aureus*, and 7 mm for *P. aeruginosa*. Overall, this research highlights the potential of activated carbon-based photocatalysts in addressing critical environmental challenges through efficient pollutant removal and antimicrobial action, contributing to sustainable WW treatment solutions. The findings will be very advantageous in developing an efficient wastewater treatment process, evaluating its upscaling potential, and serving as a framework for field application.

KEYWORDS

industrial wastewater treatment, apricot kernel shell, antimicrobial activity, green synthesis, photo-catalyst, activated carbon, Ag₂O

1 Introduction

Fostering a balanced coexistence between humanity and nature is a crucial objective for the sustainable progress of humankind. Within this endeavor, advancing the healthy and eco-friendly recycling of water resources stands as a vital component in the global pursuit of green and sustainable development (Yu et al., 2024). The presence of industrial byproducts in water bodies pose a significant threat to human health, as they have been detected in the food supply chain, including vegetables, fruits, and drinking waste (Chauhan et al., 2019; Eslami et al., 2020; An et al., 2024). The pharmaceutical industry has emerged as one of the vital contributors of this trend, with increased accessibility and affordability of drugs leading to a global annual usage growth rate of 11.9% in countries such as the USA, France, Japan, the UK, Spain, and Italy (Kaur et al., 2016; Eslami et al., 2020). A critical downside of this vast utilization of pharmaceutical substances is their unlimited discharge into both terrestrial and marine ecosystems (Chauhan et al., 2019). Pharmaceutical chemicals typically enter natural water systems through runoff from various non-point sources, including agricultural activities and effluents from static water supplies, such as hospital and municipal wastewater treatment plants (Ruziwa et al., 2023). The presence of pharmaceutical compounds in drinking water can originate from several sources, including pharmaceutical manufacturing, production processes, and both human and veterinary use (Kanakaraju et al., 2018). In light of these issues, it is essential to remove pharmaceutical compounds from water to mitigate their potential adverse effects on human health and the environment.

Aside from pharmaceutical wastewater (WW), another major concern is the presence of harmful bacteria in water bodies (Khan et al., 2021). The literature has demonstrated the dynamic nature of antimicrobial resistance in a set of pathogenic microbes (Devi et al., 2022), making it crucial to examine anti-microbial treatment methods of WW, especially for pathogenic and antibiotic-resistant bacteria (Rani et al., 2023).

Several conventional WW treatment methods such as activated sludge, adsorption, ozonation, constructed wetlands, and microalgae, have been reported for the removal of pharmaceutical compounds (Chauhan et al., 2019). While biological treatment methods are widely used for industrial WW management, techniques like activated sludge and trickling filters have proven ineffective for pharmaceutical WW, often resulting in its release into the environment and ongoing pollution of surface water, soil, and groundwater (Jureczko and Przystaś (2024)). Moreover, conventional biological WWT systems

are often inadequate for completely removing refractory toxins from pharmaceutical WW. While the main methods for treating pharmaceutical WW include both biological and physicochemical approaches, biological methods tend to be more cost-effective but are less efficient in addressing carbon-based pollutants present in the WW.

In recent years, photocatalysis has emerged as a promising technology for addressing energy challenges and mitigating environmental pollution (Lanjwani et al., 2024; Krishnan et al., 2024; Nawaz et al., 2023; 2024; 2025). Photocatalysts have numerous exceptional features, including great stability, nontoxicity, and photocatalytic degradation capability (Anjum et al., 2018a; 2018b; 2023; Wassie et al., 2024). Titanium dioxide (TiO₂) semiconductor is one of the most studied materials in heterogeneous catalysis (Anjum et al., 2019; Ranjitha et al., 2025). The TiO₂ based photocatalysis has demonstrated significant effectiveness in degrading organic and biological pollutants in WW (Lopez-Iscoa et al., 2018; Eldoma et al., 2024; Rakkini et al., 2024). The photocatalytic efficiency of TiO₂ is attributed to its unique photoelectric properties and electronic structure. The principle behind its photocatalytic activity is explained through band theory, where the catalyst is activated by continuous light exposure with energy equal to or greater than its band gap energy, leading to the formation of electron-hole pairs that facilitate the oxidation and reduction of pollutants.

Although, photocatalysts have exceptional efficiency for various applications and might be further improved for wastewater treatment, notably in the degradation of organic contaminants and inorganic heavy metal ion concentrations (Manogaran et al., 2024), and textile dyes (Selvam et al., 2022; Liu et al., 2025). Various studies have focused on metal oxides such as TiO₂ and ZnO. According to studies, ZnO is an important semiconducting photocatalyst due to its photosensitivity, low toxicity, stability, outstanding electron mobility, availability, and cost-effectiveness (Sultana et al., 2023; Ramasubramanian et al., 2023; Krobthong et al., 2024). However, the rapid recombination of electron-hole pairs in its structure restricts its photocatalytic potential (Li et al., 2015; Yi et al., 2023; Krobthong et al., 2024). Thus, minimizing recombination and stimulating carrier migration in photocatalysts may provide a solution to this problem. Such improvements could be obtained via the development of composite structures, such as using activated carbon and Ag-based photocatalysts. Activated carbon is one of the most generally utilized materials in WW treatment due to its unique porous structure and large surface area, and it

is frequently employed for organic pollutants. Furthermore, activated carbon has been proposed as an effective loading for semiconductor materials in the removal of organic chemicals (Thirumoolan et al., 2024). Similarly, silver-based photocatalysts have attracted interest for their catalytic, biomedical, water-splitting and sensing characteristics. Ag photocatalysts are known for their remarkable antibacterial and photocatalytic properties. They produce silver ions (Ag^+) that disrupt microbial respiratory chains, causing cell death (Gupta et al., 2024). Subramaniam et al. (2022) used eco-friendly synthesized Ag nanoparticles for the degradation of methylene blue radioactive dye and achieved a 96% photocatalytic degradation within 90 min. In Recently, Taghizadeh-Lendeh et al. (2024) developed Activated carbon modified with ZnO/TiO_2 catalyst for use in the photocatalytic reduction of refinery WW. The incorporation of AC into ZnO/TiO_2 has improved process efficiency and quality, resulting in increased productivity during WW treatment.

In the above context, the present study was designed with the objective of developing a photocatalyst with multiple applications, such as the removal of dyes, treatment of pharmaceutical WW, and microbial disinfection. This work pioneers transforming apricot kernel shell, an agricultural waste, into a multifunctional photocatalyst for wastewater treatment and antibacterial purposes. Unlike traditional photocatalysts, which require UV activation, the synthesized material was designed with the aim to activate in visible light, making it more energy-efficient and valuable in real-world applications. A novel carbon-based (apricot kernel shell activated carbon) modified material ($\text{AC}/\text{Ag}_2\text{O}/\text{ZnO}$) photocatalyst was synthesized. This study is the first to use apricot kernel shells with $\text{Ag}_2\text{O}/\text{ZnO}$ to develop a visible light-active photocatalyst for the treatment of pharmaceutical WW. This research will assist in developing advanced applications and may lead to breakthroughs in the field of photocatalysis. This study not only introduces a green agro-waste valorization technique but also advances the development of multifunction photocatalysts for practical wastewater treatment applications.

2 Materials and methods

2.1 Sampling and characterization of pharmaceutical wastewater

WW samples were taken from a Pharmaceutical Industry located in Islamabad, Pakistan (name withheld owing to lack of authorization). Samples were obtained from the end of the waste pipe and stored in a sterile container with a capacity of 1.5 L. Over a month, two samples were collected at different times to ensure variability in the data. Samples were carried to the lab in an icebox and maintained at 4°C , until analysis. The physico-chemical properties of the collected sample are mentioned in Table 1.

2.2 Chemicals

The chemical used in the fabrication of the photocatalysts were silver nitrate (AgNO_3), zinc sulphate heptahydrate ($\text{ZnSO}_4 \cdot 7\text{H}_2\text{O}$), and sodium hydroxide (NaOH). The azo dye Reactive Black was prepared by dissolving a measured amount in distilled water to create a dye solution for subsequent experiments.

TABLE 1 Physico-chemical characterization of pharmaceutical waste.

Parameters	Units	Values
COD	mg L^{-1}	1,283.5
TDS	mg L^{-1}	1,208
TSS	mg L^{-1}	45.14
Volatile Solids	mg L^{-1}	32.14
TFS (mg L^{-1})	mg L^{-1}	14.14
Turbidity	NTU	102
pH	-	6.8
EC	($\mu\text{s cm}^{-1}$)	985
COD	(mg L^{-1})	1,283.5

2.3 Synthesis of activated carbon and photocatalysts

2.3.1 Synthesis of apricot kernel shell activated carbon

Apricot kernel shells were harvested from trees in Khaplu, Gilgit Baltistan. The shells were thoroughly washed with water multiple times to remove impurities, then air-dried at room temperature for 24 h. The dried apricot kernel shells were placed in a digital oven set at 105°C for 2 h to eliminate any remaining moisture. The dried apricot kernel shells were subjected to mechanical treatment after initial drying. A two-step crushing process was employed using a powder grinder machine, with each milling cycle lasting 2 min, followed by a 10–20 s break to prevent overheating. The ground material was then sieved through a mesh with hole sizes of 12 or 16 to obtain uniform particle sizes.

For activation, 3 g of the ground apricot kernel shell powder was added to 100 mL of zinc chloride (ZnCl) solution. The mixture was milled and transferred into ceramic crucibles, then placed in an electric furnace at 550°C for a carbonization period of 2 h. After carbonization, the product was washed multiple times with distilled water and 10% hydrochloric acid to remove organic residues. Finally, the material was treated with phosphoric acid (H_3PO_4) and nitric acid (HNO_3) solutions before being dried at 110°C for 12 h.

2.3.2 Synthesis of $\text{AC}/\text{Ag}_2\text{O}/\text{ZnO}$ composite

$\text{AC}/\text{Ag}_2\text{O}/\text{ZnO}$ composite preparation was carried out in several sequential phases. First, a 500 mL beaker was filled with 3 g of activated carbon and 100 mL of distilled water, which was stirred continuously. Concurrently, a 50 mL solution of 0.1 M sodium hydroxide (NaOH) was prepared and added to the activated carbon solution while stirring at a temperature of 55°C . In a separate beaker, 2 g of Ag_2O was added to 100 mL of distilled water under magnetic stirring conditions, and this solution was stirred for 2 h on a hot plate magnet-stirrer to ensure complete dissolution. Similarly, another beaker contained 2 g of ZnO mixed with 100 mL of distilled water, which was also stirred under the same conditions for 2 h.

After the dissolution processes, a total of 200 mL of the NaOH solution was added to the AC mixture along with the Ag_2O and ZnO

solutions simultaneously. The combined solution was allowed to react for 24 h, during which time sediment formed at the bottom of the beaker. To remove unreacted materials, including excess nitrate and hydrate, the resulting nanocomposite was rinsed multiple times with distilled water. The washed nanocomposite was then dried in an oven at 70°C for 24 h. The final AC/Ag₂O/ZnO composite was subsequently utilized for the degradation of pharmaceutical WW.

For preparation of ZnO, a traditional sol-gel process was employed. A total of 2.196 g (0.01 mol) of zinc sulfate heptahydrate was dissolved in 60 mL of distilled water and stirred at 60°C for 30 min to produce a homogeneous solution. A separate solution containing 0.8529 g of sodium hydroxide dissolved in 50 mL of water was prepared as a 0.1 M NaOH solution and added to the zinc solution while stirring continuously for an additional 2 h. The resulting solid product was filtered out, washed with ethanol, acetone, and distilled water, and then dried at 80°C for 6 hours.

The synthesis of Ag₂O involved preparing a solution containing 0.1 M silver nitrate (AgNO₃) by dissolving appropriate amounts in 100 mL of distilled water. Concurrently, 50 mL of a 0.1 M NaOH solution was added to the silver nitrate solution while maintaining a temperature of 30°C under constant stirring for 2 hours. The Ag₂O precipitate formed during this process was recovered using vacuum filtration and washed thoroughly with ethanol and distilled water before being dried at 70°C for 6 hours.

2.4 Characterization of synthesized materials

The AC/Ag₂O/ZnO nanocomposite and powdered apricot kernel shell were characterized using Fourier-transform infrared spectroscopy (FTIR). Background correction was employed to eliminate the interference peaks from carbon dioxide and atmospheric moisture. The spectra were recorded in the range of 500–4,000 cm⁻¹ with a resolution of 4.0 cm⁻¹ to ensure accurate spectral lines. Additionally, X-ray diffraction (XRD) patterns of all photocatalysts were obtained using a diffractometer equipped with Cu-Kα radiation, with a 2θ range of 10°–90°.

2.5 Experimental setup

A series of three experiments were performed in the present study to analyze the multi-environmental application of synthesized photocatalyst. Photocatalytic experiments were performed on azo dye reactive black under varying operating conditions such as catalyst dose, pH and pollutant concentration. In second experiment, the photocatalyst was applied to real WW containing pharmaceutical active compounds under optimized conditions where the changes in chemical oxygen demand (COD) used to assess photocatalytic efficiency. Finally, in third experiment the antimicrobial activity of the synthesized photocatalyst was tested using various common pathogenic microorganism.

2.5.1 Photocatalytic degradation of azo dye reactive black (Exp. I)

The photocatalytic activity of synthesized AC/Ag₂O/ZnO composite was evaluated under direct sunlight exposure. A stock

solution of 200 mg/L was prepared by dissolving an measured amount of Reactive Black Azo Dye in distilled water. The reaction was conducted in a 250 mL quartz beaker with a working volume of 200 mL and a measured amount of catalyst was added while continuous stirring and supplying air. The effects of pH levels (3.0–9.0), catalyst dose (0.25 g/L, 0.5 g/L and 0.75 g/L) and pollutant concentrations (5 mg/L, 10 mg/L, and 15 mg/L) on the photocatalytic activity of AC/Ag₂O/ZnO were studied. Prior to initiating photocatalysis, the dye and catalyst solution were allowed to equilibrate in the dark for 30 min to facilitate adsorption. The photocatalysis reaction commenced upon exposing the solution to sunlight, with a distance of 13.84 cm maintained between the light source and reactor. The reaction mixture was continuously stirred at 550 rpm throughout the process. After each reaction period, photocatalyst materials were separated from the sample by centrifugation at 10,000 rpm for 15 min. The concentration of the dye in degrading solutions was determined using a UV-visible spectrophotometer (UV-5100) at wavelengths ranging from 520 nm to 590 nm. The percentage degradation of dye in water was calculated using the following formula (Equation 1):

$$\text{Degradation (\%)} = \frac{C_i - C_t}{C_i} \times 100 \quad (1)$$

To assess the stability and reusability, the photocatalyst was removed from the solution after the first run, cleaned with acetone, ethanol, and distilled water, and then dried at 60°C for 6 h before being reused in subsequent runs (Senasu et al., 2021). The same process was repeated for four cycles to evaluate the reusability of the photocatalyst.

2.5.2 Photocatalytic treatment of pharmaceutical WW (Exp. II)

The photocatalytic activity was also tested on pharmaceutical WW under direct sunlight exposure. The pharmaceutical WW was subjected to photocatalytic treatment using two photocatalysts, i.e., AC/Ag₂O/ZnO and Ag₂O/ZnO (without Activated Carbon) in comparison to photolysis (without catalyst) treatment. The reaction was conducted in a 500 mL beaker with working volume of 400 mL and a catalyst dose of 0.5 g/L while ensuring continuous aeration and stirring. Samples were collected at regular intervals for analysis. Prior to starting the photocatalysis reaction, the mixture of WW and catalyst was kept in the dark for 30 min in order to establish an adsorption equilibrium. Following this period, the system was exposed to visible sun light to initiate the photocatalytic reaction. The WW samples were collected at different intervals and treatment efficiency was measured by analyzing COD. Furthermore, the effect of photocatalysis was also assessed by analyzing other water quality parameters such as pH, EC, TSS, TDS, VS, COD, and heavy metals after completion of process.

2.5.3 Antimicrobial activity (Exp. III)

The antibacterial activity of AC/Ag₂O/ZnO was evaluated by agar well diffusion assays (Dawar et al., 2023) against three microorganisms, i.e., *Escherichia coli* (Gram-ve) and *Staphylococcus aureus* (Gram + ve), as well as *Pseudomonas aeruginosa* (Gram-ve). These microbial strains were acquired

TABLE 2 Pathogenic bacterial Strain used for antimicrobial activity test.

Bacterial strain	Nature	Source
<i>Escherichia coli</i>	Gram negative	Islamic International University Islamabad
<i>Staphylococcus aureus</i>	Gram positive	Pathology Lab Holy Family Hospital Rawalpindi
<i>Pseudomonas aeruginosa</i>	Gram negative	Pathology Lab Holy Family Hospital Rawalpindi

from different sources as mentioned in Table 2. Bacterial strains were subculture in nutrient agar plates, where zones of inhibition (ZOI) were measured after adding 50 mg of AC/Ag₂O/ZnO into wells created using a sterile metallic borer with diameters ranging from 4 to 8 mm. The plates were incubated for 24 h at 37°C under light conditions; additional assays were conducted under dark conditions for comparative analysis.

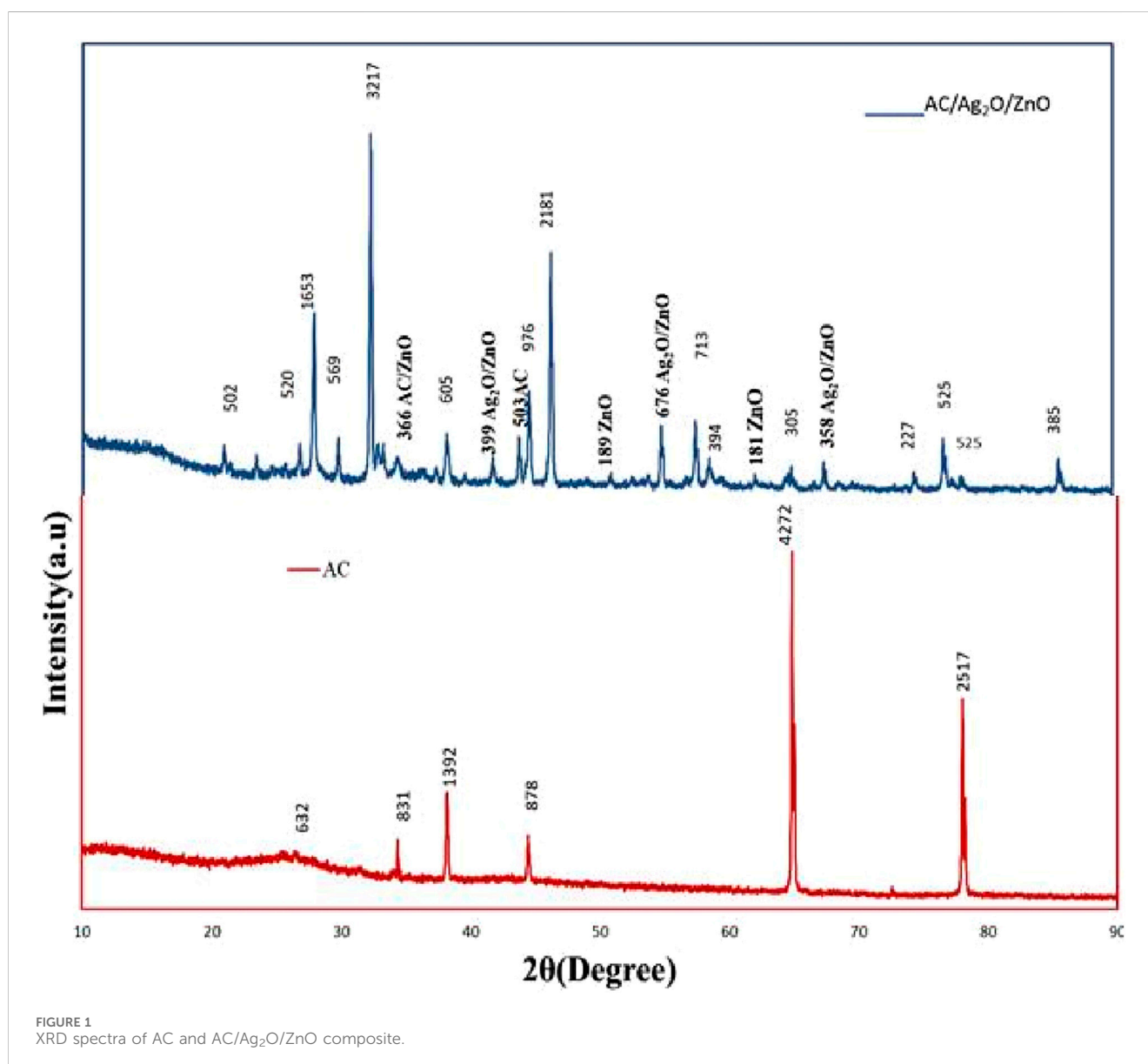
2.6 Analysis

The water quality parameters such as COD, TSS, VS, TDS, FS, pH, and EC were analysed using the standard method of APHA 2005. Dye concentrations was measured using a UV-visible spectrophotometer, while heavy metal concentrations were assessed using ICP-OES. The antimicrobial activity was analyzed by well diffusion method by measuring ZOI.

3 Results and discussion

3.1 Characterization of photocatalysts

To identify the composition of the newly developed photocatalyst material, X-ray diffraction was performed to identify the peaks within the 2θ range of 10°–90° range, a standard range widely used in the literature (Haider et al., 2023;



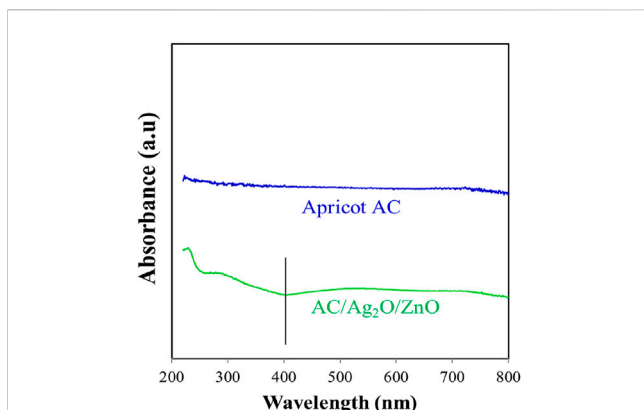


FIGURE 2 UV-Visible spectra of AC and AC/Ag₂O/ZnO composite.

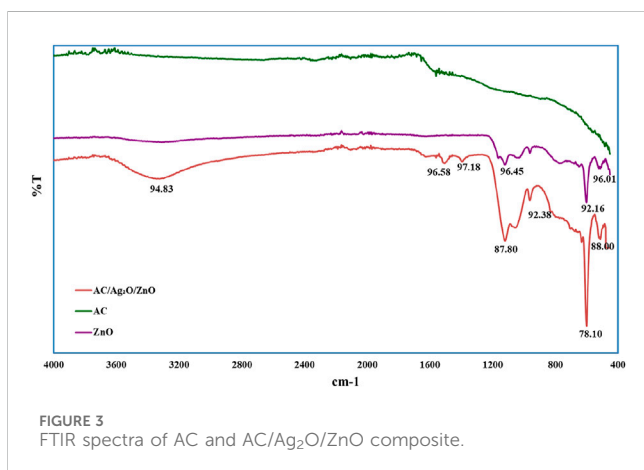


FIGURE 3 FTIR spectra of AC and AC/Ag₂O/ZnO composite.

Rao et al., 2024). The XRD patterns of the prepared AC/Ag₂O/ZnO composite and AC are illustrated in Figure 1. In the XRD spectra of AC/Ag₂O/ZnO nanocomposite, distinct peaks at 2θ values of 27.97°, 32.37°, 38.25°, 44.63°, 46.35°, 54.91°, 57.58°, 76.80°, corresponds to the (1,653), (3,217), (605), (976), (2,181), (676), (713), (525) planes, respectively. These results confirm the formation of Ag₂O, which is identified as having an orthorhombic crystal system according to JCPDS# 01-077-1829. The ZnO spectra revealed additional peaks at 2θ values of 31.84, 34.41, 36.36, 47.65, 56.61, 62.86, 66.3°, 67.94, and 69.19, corresponding to the reflection planes 100, 002, 101, 102, 110, 103, 200, 112, and 201, respectively. Additionally, the 102 and 110 planes of the hexagonal ZnO phase were indexed to two diffraction peaks at $2\theta = 47.58$ and 56.33 . Jankovic et al. (2019) reported that raw apricot kernel shell biomass exhibited two prominent peaks at 22.40° and 34.60°. The peak at 22.40° is indicative of amorphous carbon, while the smaller peak at 34.60° suggests the presence of cellulose I structure due to the (004) lattice plane, which can be attributed to the breaking of C-C bonds during processing.

The UV-DRS absorption spectrum of the apricot activated carbon and its composite with Ag₂O/ZnO is represented in Figure 2. It was observed that the simple Apricot AC showed limited solar light utilization efficiency due to its biomass origin,

TABLE 3 Proximate analysis of apricot kernel shell.

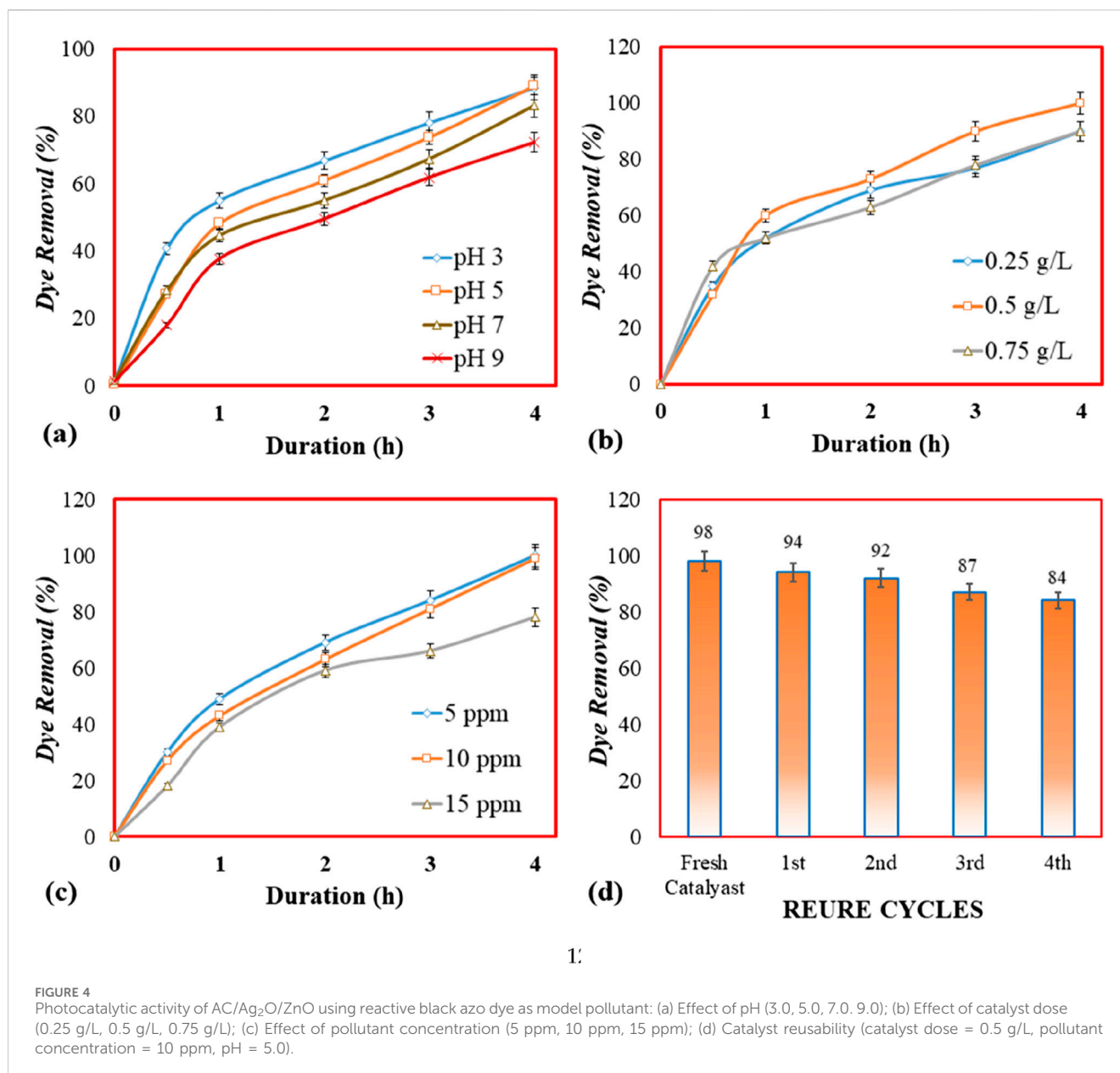
Proximate analysis parameters	Ultimate analysis (wt%) apricot kernel shell
Bulk Density	0.75
Moisture	9.65
Fixed Carbon	15.43
Volatile matter	72.00
pH	3.09
Ash Content	0.87

which likely results in a lower band gap energy. However, significant changes in the absorption band were noted after modification; this aligns with findings reported in previous studies (Kumar et al., 2024). The visible light absorption region of the AC/Ag₂O/ZnO composite was markedly enhanced beyond 400 nm, attributed to the high sensitivity of Ag₂O to visible light (Zang et al., 2022).

To evaluate presence of functional groups infrared (IR) spectra were obtained in the 4,000–400 cm⁻¹ range following established protocols (Devi et al., 2023). In Figure 3, it can be observed that the apricot kernel shell AC exhibited a broad band at 3,722 cm⁻¹ corresponding to hydroxyl group absorption from polysaccharides (Figure 3). In contrast, the AC/Ag₂O/ZnO composite displayed characteristic peaks at approximately 772 cm⁻¹, which may be associated with Zn-O bonds (Anjum et al., 2017). The vibrational modes of Ag₂O were indicated by two additional broad peaks located at 960 cm⁻¹ and 1,057 cm⁻¹. Furthermore, two vibrational bands around 1,633 cm⁻¹ and 3,439 cm⁻¹, representing O-H bending and O-H stretching from water respectively, were clearly present in all catalysts. The ZnO catalysts exhibited strong peaks at approximately 451 cm⁻¹ due to Zn-O linkages (Senasu et al., 2021). Additionally, aromatic skeletal vibrations observed at around 1,585 cm⁻¹ and 1,505 cm⁻¹ in the spectra of raw apricot kernel shells were completely eliminated in the carbonized shells, indicating a transformation in phenyl chains as reported by Jankovic et al. (2019).

3.2 Proximate analysis of apricot kernel shell

The proximate analysis of the apricot kernel shell is summarized in Table 3. The pH of activated carbon was 3.9 and ash content was found to be 0.87%. The bulk density of the activated carbon was 0.75 g/cm³. The volatile matter content was 72% which represents the presence of significant amount of organics. These findings align with results reported by Jankovic et al. (2019). It was observed that the moisture content of biomass was very low, i.e. 9.71%. Moisture content of biomass is critical for effective synthesis of activated carbon through thermal process. Excess moisture can increase heat energy consumption during thermal treatment as heat energy is primarily used to evaporate water rather than to raise the biomass temperature (Fonseca et al., 2019). In apricot kernel shells, the ash content 0.94% was recorded while the volatile matter was quite



1:

FIGURE 4

Photocatalytic activity of AC/Ag₂O/ZnO using reactive black azo dye as model pollutant: (a) Effect of pH (3.0, 5.0, 7.0, 9.0); (b) Effect of catalyst dose (0.25 g/L, 0.5 g/L, 0.75 g/L); (c) Effect of pollutant concentration (5 ppm, 10 ppm, 15 ppm); (d) Catalyst reusability (catalyst dose = 0.5 g/L, pollutant concentration = 10 ppm, pH = 5.0).

higher (72%). Canales-Flores and Prieto-Garcia (2016) noted that the VM values for apricot kernel shells fall within the range observed for other precursors used in activated carbon production (69%–84%). The high VM concentration is advantageous for the carbonization process, as the controlled release of volatile matter enhances the carbon content of the precursor (Deenik et al., 2010).

3.3 Photocatalytic activity

The photocatalytic activity of the synthesized photocatalyst was evaluated using Azo Dye Reactive Black as a model pollutant. A series of experiments were conducted to optimize various operating conditions such as pH, pollutant concentration and, pH under solar light irradiation.

3.3.1 Effect of solution pH on photocatalytic activity

The solution pH is one of the important regulating factors for the production of OH[•] radicals needed for the processing of photocatalysis (Yang et al., 2013). The impact of pH was examined by varying initial pH (3.0–9.0). The results showed that the azo dye removal was 37% during the first 30 min of the dark period at pH 5 (Figure 4a). This removal occurred as a result of the adsorption of azo dye over the surface of AC/Ag₂O/ZnO nanocomposite. It is reported that the adsorption is promoted by acidic and neutral conditions, notably at a pH of around 5. In the case of photocatalysis under light exposure after 30 min, a significant boost in dye removal was observed where the maximum removal was achieved up to 88.5% and 89% after 4 h at pH 3.0 and pH 5.0, respectively. The inclusion of activated carbon provided the catalyst with unique properties, including increased visible light absorption, mobility of charge

carriers, and the capacity to function as an electron donor (Tian et al., 2022). Thus, compared to other pH ranges, an acidic pH of 5.0 was optimum for increased photocatalytic degradation of azo dye by AC/Ag₂O/ZnO under visible light. These findings are consistent with previous studies, e.g., Kweinor Tetteh et al. (2021) achieved the maximum azo dye (Basic Blue 41) removal at pH 6 with AC-TiO₂, demonstrating the optimal degradation of azo dyes under slightly acidic conditions, possibly due to enhanced adsorption and photocatalysis at this pH.

3.3.2 Effect of catalyst dose

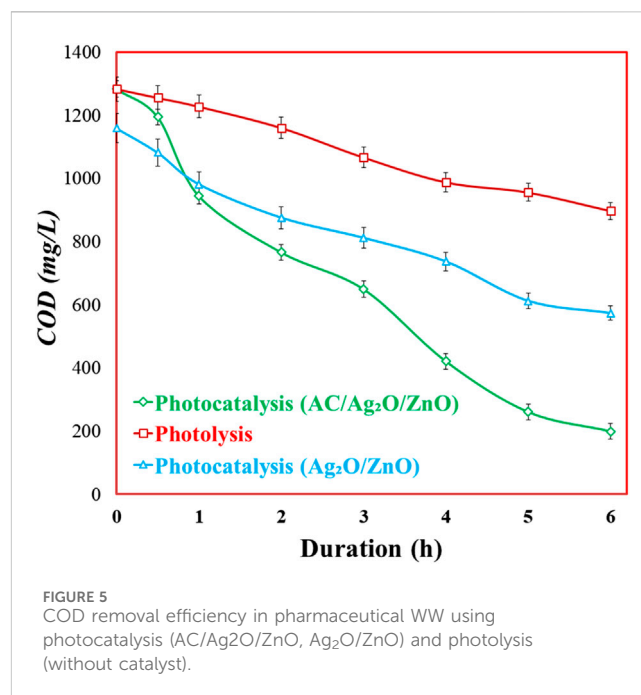
The effect of the varying catalyst dosage on the removal of reactive black azo dye from water is represented in (Figure 4b). It has been observed that with the increase in photocatalyst dose from 0.25 g/L to 0.5 g/L, the dye removal efficiency of dye also increased. The maximum dye removal was achieved with 0.5 g/L of AC/Ag₂O/ZnO catalyst, where 99% of dye removal was achieved. This is due to the fact that at the higher dose of catalyst, more and more active sites are available for the dye to adsorb on the catalyst surface and subsequently degrade due to the photocatalysis mechanism. With a further increase in catalyst dose to 0.75 g/L, the dye removal efficiency decreased. Excess catalyst load may lead to particle agglomeration, which possibly reduces the accessible surface area for dye adsorption (Akpan and Hameed, 2009). Therefore, at the optimal catalyst dose (0.5 g/L), the molecules dye efficiently adsorb on the catalyst surface. Further, a high catalyst dose may disturb the adsorption-desorption equilibrium, limiting the interaction between the dye molecules and photocatalytically active sites (Wang et al., 2021).

3.3.3 Effect of pollutant concentration

The effect of pollutant concentration on photocatalytic degradation of azo dyes was investigated at different concentrations (5 ppm, 10 ppm, and 15 ppm) using optimum AC/Ag₂O/ZnO dose of g/L and pH 5.0 (Figure 4c). It was observed the maximum dye removal efficiency of 99% was attained at lowest dye concentration of 5 ppm, followed by 98% at 10 ppm and less than 90% at 15 ppm. Thus, maximum optimal dye concentration was determined to be 10 ppm. The highest removal efficacy up to 98% at 10 ppm (dye concentration) surpasses the outcomes of previous research using traditional TiO₂ photocatalysts, which typically recorded 85%–95% of pollutant removal. The lowering in dye removal efficiency at higher concentration (15 ppm) could be due to the saturation and unavailability of active sites at catalyst surface, which increase the competition for reactive hydroxyl radicals (essential for degradation). Previous studies such as (Mohamed et al., 2024; Hemmatzadeh et al., 2024) also reported a similar trend, where they observed reduced photocatalytic efficiency at higher pollutant concentrations. This can be also be explained by the possibility that an increase in pollutant concentration might lead to a fall in optical density, which would increase the viscosity of the solution and limit photon penetration while enhancing the photon length route, resulting in less azo dye degradation (Chen et al., 2024).

3.3.4 Reusability of the catalyst

The reusability of used AC/Ag₂O/ZnO was examined for the degradation of reactive black azo dye under optimum operating conditions (Figure 4d). After the first use, the catalyst was recycled by washing properly with deionized water and dried in an oven for 12 h at 60 °C. In the same way, the catalyst was recycled and reused



four times under optimum conditions. It was noted that the catalysts' efficiency remained steady during all four runs, where the dye removal efficacy was up to 86% even after the fourth time catalyst reuse. The slight decrease in photocatalytic activity may be due to the intermediate products connected to the catalyst surface preventing dye molecules from interacting with the AC/Ag₂O/ZnO surface. Previously, several investigations found that the photocatalyst may be used repeatedly with just a minor loss of photocatalytic activity (Zahedifar and Seyedi, 2022; Hutsul et al., 2022). In order to improve the stability and performance over multiple cycles, there are several strategies that can be adopted in future research, such as moderate thermal treatment, which can remove surface adsorbed substances, chemical-based washing like mild oxidizing agents, can regenerate active sites, and electrochemical treatment by applying a small voltage can restore surface properties. Overall, it can be concluded that AC/Ag₂O/ZnO is considerably stable and could be a flexible choice for the treatment of polluted water without any necessity for disposal.

3.4 Photocatalytic treatment of real pharmaceutical WW

3.4.1 COD removal efficiency

In this phase, the pharmaceutical WW was subjected to photocatalytic treatment using two photocatalysts, i.e., AC/Ag₂O/ZnO and Ag₂O/ZnO (without activated carbon), in comparison to photolysis (without catalyst) treatment. The treatment efficiency was estimated by measuring COD, basic water quality parameters, and heavy metals concentration. The results regarding COD reduction over the photocatalysis of 6 h are presented in Figure 5. The reduction of COD is directly linked to the mineralization of organic pollutants into CO₂ and H₂O molecules. It was observed that the highest COD reduction from 1,283.5 mg/L to 199 mg/L was achieved with AC/Ag₂O/ZnO,

TABLE 4 Effect of photocatalysis on heavy metal concentration in pharmaceutical WW.

Heavy metals	RAW WW (mg-L ⁻¹)	*PL WW (mg-L ⁻¹)	**PC WW (mg-L ⁻¹)
Al	2.33	2.08	2.04
As	0.10	0.5	0.04
Cd	0.21	0.19	0.16
Co	ND	ND	ND
Cr	ND	ND	ND
Fe	0.33	0.20	ND
K	3.48	2.98	2.31
Ni	0.01	0.01	0.00
Pb	1.29	1.00	0.93

*PL: photolysis, **PC: photocatalysis, ND: not detected.

TABLE 5 Pharmaceutical WW treatment efficiency.

Parameters	Before treatment (raw WW)	After photocatalytic (AC/Ag ₂ O/ZnO) treatment	Percentage change
COD (mg L ⁻¹)	1,283.5	199	84.5
TDS (mg L ⁻¹)	1,200	197	83.6
TSS (mg L ⁻¹)	45.14	18.3	59.5
VS (mg L ⁻¹)	32.14	10.3	68.0
FS (mg L ⁻¹)	14.14	5.39	61.9
Turbidity (NTU)	102	86.7	15.0
pH	6.8	5.2	-

followed by Ag₂O/ZnO (1,159 mg/L to 573 mg/L) and photolysis (1,284 mg/L to 897 mg/L). The superior treatment performance of AC/Ag₂O/ZnO can be attributed to the synergistic effect of ZnO and Ag₂O that assisted in charge separation and efficient generation of reactive oxygen species in water, resulting in the effective removal of organic pollutants (Liu et al., 2022). On the other hand, AC offers extra sites for adsorption and enhances the interaction between photocatalysts and pollutants. The findings of present study are consistent with Abdullah et al. (2023) where the activated carbon (AC)-based TiO₂ photocatalyst achieved a higher COD removal (99%) compared to that with AC or TiO₂ alone. Overall, these outcomes underscore the potential of AC/Ag₂O/ZnO as a highly active photocatalyst for treating pharmaceutical WW, contributing to a sustainable solution for controlling organic pollution in industrial effluent.

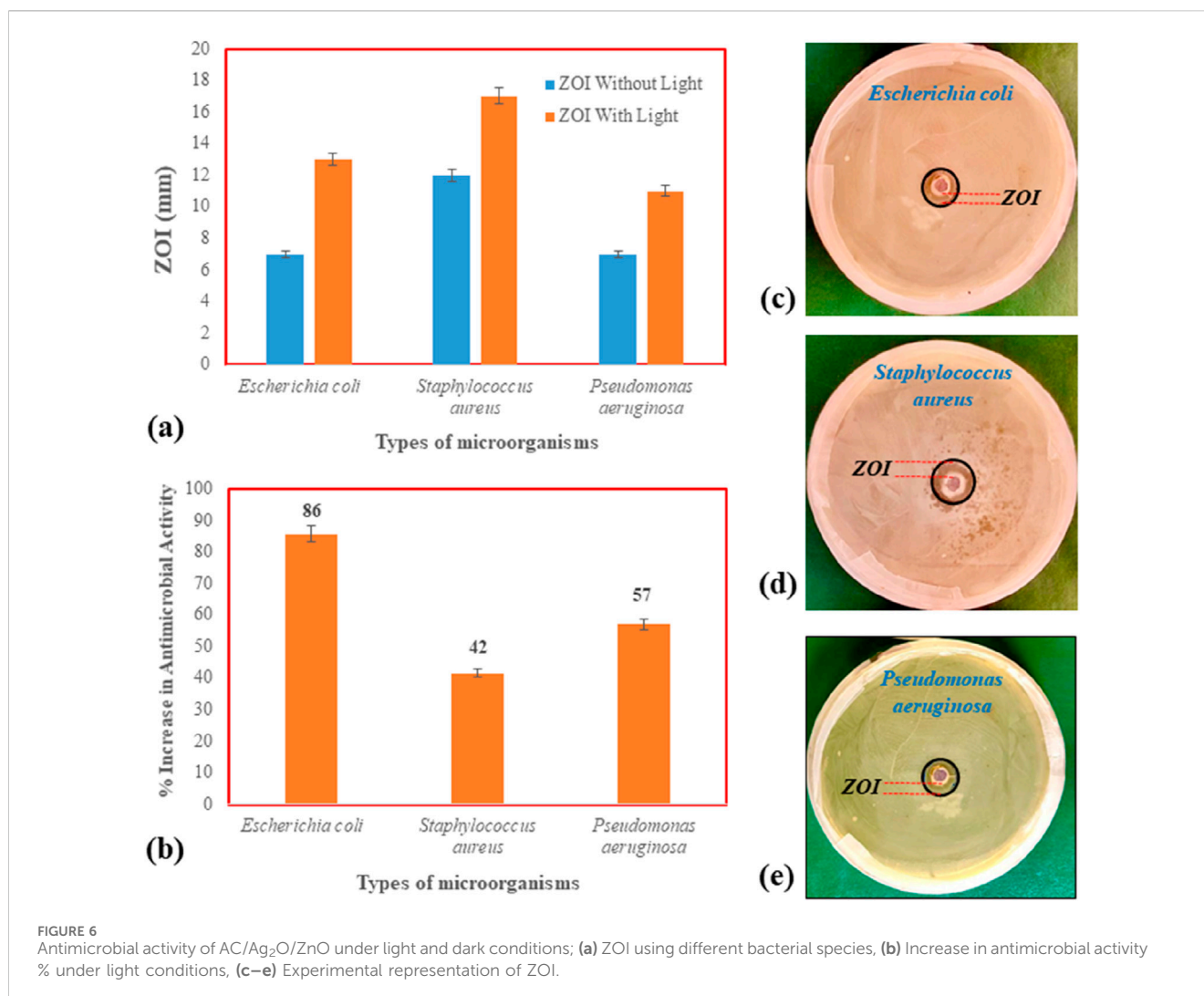
3.4.2 Removal of metals

The removal of metals from pharmaceutical WW by AC/Ag₂O/ZnO photocatalysis is described in Table 4. It was found that the AC/Ag₂O/ZnO catalyst does of 0.5 g/L and pH 5.0, significantly reduced the metals such as Al, Cd, Fe and Pb have reduced by greater concentrations by photocatalysis compared to photolysis (without catalyst). For Al, the concentration was reduced to 2.04 ppm in photocatalysis from 2.33 ppm, Cd 0.16 ppm from 0.21 ppm, Fe

0 ppm from 0.33 ppm, and Pb 0.93 ppm from 1.29 ppm, respectively. In the case of K, photocatalysis significantly reduced the concentration to 2.31 ppm from 3.48 ppm. The Co and Cr were not detected in both raw and treated wastewater. This removal of metals from WW is possibly due to the adsorption over the surface of photocatalysts containing activated carbon (Shukor et al., 2019). As the present study was conducted under an acidic pH range (5.0), Srivastava et al. (2015) also reported that adsorption of the heavy metals from WW is greatly influenced by pH, where they found that Zn (II) removal was highest at pH 5.5, though with rise in pH, the removal becomes less effective. Similarly, in another study (Lingamdinne et al., 2016), Pb (II) and Cr (III) were reduced by 93% and 99.6%, respectively, at pH values of 6.0 and 4.0.

3.4.3 Pharmaceutical WW treatment efficiency

The effectiveness of pharmaceutical wastewater treatment using AC/Ag₂O/ZnO is summarized in Table 5. The COD values showed a substantial decrease from 1,284 mg L to 1 to 199 mg L⁻¹, indicating a significant reduction (84.5%) in overall organic pollutants in WW. The TDS and TSS were reduced from 1,200 mg L⁻¹ to 197 mg L⁻¹ and 45.14 mg L⁻¹ to 18.3 mg L⁻¹, showing treatment efficiency of 83.6% and 59.5%, respectively. Similarly, VS exhibits a significant reduction from 32.14 mg L⁻¹ to 10.3 mg L⁻¹, respectively. In the case of Turbidity of WW, the values decreased from 102 NTU to 86.7 NTU, and a slight change in pH from 6.8 to 5.2, indicating slight



acidification of wastewater. Overall, the results underline the potential of photocatalytic treatment using AC/Ag₂O/ZnO photocatalyst as an effective approach for treating pharmaceutical wastewater.

3.5 Antimicrobial activity of AC/Ag₂O/ZnO

Different NPs have extensively been reported in literature for their strong antimicrobial activities. The microbial strains *E. coli*, *S. aureus*, and *P. aeruginosa* were used to assess the antimicrobial activity of the AC/Ag₂O/ZnO composite, which demonstrated greater effectiveness under light conditions compared to dark conditions (Figure 6). Interestingly the stronger ZOI was observed for Gram positive bacteria that is *S. aureus* compared to Gram negative bacteria that is *E. coli* and *P. aeruginosa*. These results are inconsistent with the previous findings of Govarthanan et al. (2020), where zinc based NPs have shown stronger antimicrobial activity against Gram positive bacteria compared to Gram negative bacteria. However, the results are in contrast to the findings of Rathinavel, et al. (2020) where the ZOI was higher for *P. aeruginosa* than *S. aureus*. Similarly, silver NPs were also found

effective against *S. aureus* and *E. coli* (Abareethan et al., 2024). One interesting finding in the current work was the effectiveness of the antimicrobial activity of AC/Ag₂O/ZnO composite in light culture media. After incubation in the dark with AC/Ag₂O/ZnO, the bacterial growth suppression appeared as a zone surrounding the well that was 7 mm in diameter for *E. coli*, 12 mm for *S. aureus*, and 7 mm for *P. aeruginosa*. While sunlight-irradiated culture medium demonstrates the bacterial ZOI expanded in diameter increasing to 13 mm with *E. coli*, 17 mm with *S. aureus*, and 11 mm with *P. aeruginosa*. It is possible that the bacterial membrane is harmed due to the photocatalytic stimulation of the catalyst and production of allowed radicals and the reactive oxygen species. The well-loaded materials significantly boosted the multi-factorial bactericidal efficiency, which inhibits bacterial growth and creates large ZOI. According to the findings, antimicrobial activity on an agar plate under light irradiation was around 15.26% greater than it was under dark-mediated response. It has been observed that that only a few *Escherichia coli* colonies persisted after being exposed to the catalyst AC/Ag₂O/ZnO under light irradiation, shows the visual difference. A comparative assessment (Table 6) showed that the antimicrobial activity of AC/Ag₂O/ZnO was comparable and significantly higher in many cases.

Based on the steps outlined by Elbasuney et al. (2023), the antibacterial mechanism of AC/Ag₂O/ZnO could involve the following phases. First, AC/Ag₂O/ZnO wraps around the microorganisms and attaches to their outer surface, causing the ion to rupture the membrane. Then, the internal cell organelles are dispersed in the microbial cell. The production of reactive organic species causes oxidative stress, which eventually leads to damage to the cell. Finally, materials prohibit ions from being transferred to and from microbial cells, resulting in cell death.

4 Conclusion

In the present study, the apricot kernel shells were successfully utilized for the synthesis of AC-based novel photocatalyst. The synthesized AC/Ag₂O/ZnO photocatalyst showed a high solar-light active efficiency with 99% of azo dye degradation. The effective photocatalytic property demonstrates its promising potential for treating pharmaceutical WW. The total COD removal was 84.5%, with a significant reduction in toxic metals concentration. Furthermore, high antimicrobial activity against *E. coli*, *S. aureus*, and *P. aeruginosa* showed the catalyst ability for disinfection of potential pathogenic microorganisms. Overall, the present study demonstrated the efficiency of a newly synthesized AC/Ag₂O/ZnO photocatalyst for a variety of environmental applications such as azo dyes degradation, treatment of pharmaceutical WW, and microbial disinfection. In addition to increasing the efficiency of photocatalysts, using solar light (visible light) for activation makes this method a highly economical and broader application.

Data availability statement

The original data presented in the study will be available from the corresponding author upon a reasonable request.

Author contributions

FL: Conceptualization, Data curation, Writing—original draft. FB: Investigation, Methodology, Software, Visualization,

Writing—review and editing. MA: Conceptualization, Funding acquisition, Project administration, Resources, Supervision, Writing—review and editing. SQ: Data curation, Formal Analysis, Writing—review and editing. AI: Writing—review and editing. WN: Formal Analysis, Writing—review and editing. ZR: Funding acquisition, Resources, Writing – review and editing. HU: Resources, Supervision, Writing—review and editing.

Funding

The author(s) declare that financial support was received for the research and/or publication of this article. This research was supported by the Key Research and Development Program of Zhejiang Province, China (2024C03125). The authors extend their appreciation to the Deanship of Scientific Research at King Khalid University for funding this work through Large Groups Project under grant number RGP.2/428/45.

Conflict of interest

The authors declare that the research was conducted in the absence of any commercial or financial relationships that could be construed as a potential conflict of interest.

Generative AI statement

The author(s) declare that no Generative AI was used in the creation of this manuscript.

Publisher's note

All claims expressed in this article are solely those of the authors and do not necessarily represent those of their affiliated organizations, or those of the publisher, the editors and the reviewers. Any product that may be evaluated in this article, or claim that may be made by its manufacturer, is not guaranteed or endorsed by the publisher.

References

- Abareethan, M., Sathiyapriya, R., Pavithra, M. E., Parvathy, S., Thirumalaisamy, R., Selvankumar, T., et al. (2024). Biogenic silver nanoparticles from *Solanum trilobatum* leaf extract and assessing their antioxidant and antimicrobial potential. *Chem. Phys. Impact* 9, 100771. doi:10.1016/j.chphi.2024.100771
- Abdullah, M., Iqbal, J., Rehman, M. S. U., Khalid, U., Mateen, F., Arshad, S. N., et al. (2023). Removal of ceftriaxone sodium antibiotic from pharmaceutical wastewater using an activated carbon based TiO₂ composite: adsorption and photocatalytic degradation evaluation. *Chemosphere* 317, 137834. doi:10.1016/j.chemosphere.2023.137834
- Akpan, U. G., and Hameed, B. H. (2009). Parameters affecting the photocatalytic degradation of dyes using TiO₂-based photocatalysts: a review. *J. Hazard. Mater.* 170 (2-3), 520–529. doi:10.1016/j.jhazmat.2009.05.039
- An, X., Wang, Y., Yu, C., and Hu, X. (2024). Biochar-bacteria coupling system enhanced the bioremediation of phenol wastewater-based on life cycle assessment and environmental safety analysis. *J. Hazard Mater* 480, 136414. doi:10.1016/j.jhazmat.2024.136414
- Anjum, M., Kumar, R., Abdelbasir, S. M., and Barakat, M. A. (2018a). Carbon nitride/titanium nanotubes composite for photocatalytic degradation of organics in water and sludge: pre-treatment of sludge, anaerobic digestion and biogas production. *J. Environ. Manag.* 223, 495–502. doi:10.1016/j.jenvman.2018.06.043
- Anjum, M., Kumar, R., and Barakat, M. A. (2018b). Synthesis of Cr₂O₃/C₃N₄ composite for enhancement of visible light photocatalysis and anaerobic digestion of wastewater sludge. *J. Environ. Manag.* 212, 65–76. doi:10.1016/j.jenvman.2018.02.006
- Anjum, M., Liu, W., Qadeer, S., and Khalid, A. (2023). Photocatalytic treatment of wastewater using nanoporous aerogels: opportunities and challenges. *Emerg. Tech. Treat. Toxic Metals Wastewater*, 495–523. doi:10.1016/b978-0-12-822880-7.00003-0
- Anjum, M., Miandad, R., Waqas, M., Gehany, F., and Barakat, M. A. (2019). Remediation of wastewater using various nano-materials. *Arabian J. Chem.* 12 (8), 4897–4919. doi:10.1016/j.arabjc.2016.10.004
- Anjum, M., Oves, M., Kumar, R., and Barakat, M. A. (2017). Fabrication of ZnO-ZnS/polyaniline nanohybrid for enhanced photocatalytic degradation of 2-chlorophenol and microbial contaminants in wastewater. *Int. Biodeterioration & Biodegrad.* 119, 66–77. doi:10.1016/j.ibiod.2016.10.018

- Canales-Flores, R. A., and Prieto-García, F. (2016). Activation methods of carbonaceous materials obtained from agricultural waste. *Chem. Biodivers.* 13 (3), 261–268. doi:10.1002/cbdv.201500039
- Chauhan, A., Sillu, D., and Agnihotri, S. (2019). Removal of pharmaceutical contaminants in wastewater using nanomaterials: a comprehensive review. *Curr. Drug Metab.* 20 (6), 483–505. doi:10.2174/1389200220666181127104812
- Chen, S., Chen, C., Shi, Y., Xu, X., Wang, Y., Pan, L., et al. (2024). Construction of PANI@V2O5-ZnIn2S4 Z-scheme heterojunction photocatalysts for highly effective degradation of industrial dyes and antibiotics. *J. Environ. Chem. Eng.* 12 (5), 114097. doi:10.1016/j.jece.2024.114097
- Dawar, N., Devi, J., Kumar, B., and Dubey, A. (2023). Synthesis, characterization, pharmacological screening, molecular docking, DFT, MESP, ADMET studies of transition metal (II) chelates of bidentate Schiff base ligand. *Inorg. Chem. Commun.* 151, 110567. doi:10.1016/j.inoche.2023.110567
- Deenik, J. L., McClellan, T., Uehara, G., Antal, M. J., and Campbell, S. (2010). Charcoal volatile matter content influences plant growth and soil nitrogen transformations. *Soil Sci. Soc. Am. J.* 74 (4), 1259–1270. doi:10.2136/sssaj2009.0115
- Devi, J., Kumar, B., Dubey, A., Tufail, A., and Boora, A. (2023). Exploring the antimalarial and antioxidant efficacy of transition metal (II) chelates of thiosemicarbazone ligands: spectral investigations, molecular docking, DFT, MESP and ADMET. *BioMetals* 37, 247–265. doi:10.1007/s10534-023-00546-1
- Devi, J., Kumar, S., Kumar, B., Asija, S., and Kumar, A. (2022). Synthesis, structural analysis, *in vitro* antioxidant, antimicrobial activity and molecular docking studies of transition metal complexes derived from Schiff base ligands of 4-(benzoyloxy)-2-hydroxybenzaldehyde. *Res. Chem. Intermed.* 48 (4), 1541–1576. doi:10.1007/s11164-021-04644-y
- Elbasuney, S., El-Khawaga, A. M., Elsayed, M. A., Elsaidy, A., and Correa-Duarte, M. A. (2023). Enhanced photocatalytic and antibacterial activities of novel Ag-HA bioceramic nanocatalyst for waste-water treatment. *Sci. Rep.* 13 (1), 13819. doi:10.1038/s41598-023-40970-4
- Eldoma, M. A., Alaswad, S. O., Mahmoud, M. A., Qudsieh, I. Y., Hassan, M., Bakather, O. Y., et al. (2024). Enhancing photocatalytic performance of Co-TiO₂ and Mo-TiO₂-based catalysts through defect engineering and doping: a study on the degradation of organic pollutants under UV light. *J. Photochem. Photobiol. A Chem.* 446, 115164. doi:10.1016/j.jphotochem.2023.115164
- Eslami, A., Amini, M. M., Asadi, A., Safari, A. A., and Daglioglu, N. (2020). Photocatalytic degradation of ibuprofen and naproxen in water over NS-TiO₂ coating on polycarbonate: process modeling and intermediates identification. *Inorg. Chem. Commun.* 115, 107888. doi:10.1016/j.inoche.2020.107888
- Fonseca, F. G., Funke, A., Niebel, A., Dias, A. P. S., and Dahmen, N. (2019). Moisture content as a design and operational parameter for fast pyrolysis. *J. Anal. Appl. Pyrolysis* 139, 73–86. doi:10.1016/j.jaap.2019.01.012
- Govarthanan, M., Srinivasan, P., Selvankumar, T., Janaki, V., Al-Misned, F. A., El-Serehy, H. A., et al. (2020). Utilization of funnel-shaped ivory flowers of Candelabra cactus for zinc oxide nanoparticles synthesis and their *in-vitro* anticancer and antibacterial activity. *Mater. Lett.* 273, 127951. doi:10.1016/j.matlet.2020.127951
- Gupta, S., Kumar, R., and Goel, G. (2024). Synergistic photocatalytic and antibacterial efficacies of Ag/rGO and Ag/Ag₂O/rGO nanocomposites: the impact of oxide formation and ternary heterojunction. *Mater. Today Commun.* 41, 110479. doi:10.1016/j.mtcomm.2024.110479
- Haider, S., Nawaz, R., Anjum, M., Haneef, T., Oad, V. K., Uddinkhan, S., et al. (2023). Property-performance relationship of core-shell structured black TiO₂ photocatalyst for environmental remediation. *Front. Environ. Sci. & Eng.* 17 (9), 111. doi:10.1007/s11783-023-17111-3
- Hemmatzadeh, E., Bahram, M., Anjum, M., and Dadashi, R. (2024). Photochemical modification of tea waste by tungsten oxide nanoparticle as a novel, low-cost and green photocatalyst for degradation of dye pollutant. *Spectrochimica Acta Part A: Molecular and Biomolecular Spectroscopy.* 313, 124104. doi:10.1016/j.saa.2024.124104
- Hutsul, K., Stepanova, A., Byts, O., and Ivanenko, I. (2022). Photocatalytic activity of ZnO under near-real conditions. *Mater. Today Proc.* 62, 7654–7659. doi:10.1016/j.matpr.2022.02.484
- Jankovic, B., Manić, N., Dodevski, V., Radović, I., Pijović, M., Katnić, Đ., et al. (2019). Physico-chemical characterization of carbonized apricot kernel shell as precursor for activated carbon preparation in clean technology utilization. *J. Clean. Prod.* 236, 117614. doi:10.1016/j.jclepro.2019.117614
- Jureczko, M., and Przystaś, W. (2024). Toxicity toward freshwater and marine water organisms of the cytostatic drugs bleomycin and vincristine and their binary mixture. *Sci Total Environ.* doi:10.1016/j.scitotenv.2024.173175
- Kanarakaju, D., Glass, B. D., and Oelgemöller, M. (2018). Advanced oxidation process-mediated removal of pharmaceuticals from water: a review. *J. Environ. Manag.* 219, 189–207. doi:10.1016/j.jenvman.2018.04.103
- Kaur, A., Umar, A., and Kansal, S. K. (2016). Heterogeneous photocatalytic studies of analgesic and non-steroidal anti-inflammatory drugs. *Appl. Catal. A General* 510, 134–155. doi:10.1016/j.apcata.2015.11.008
- Khan, A. H., Aziz, H. A., Khan, N. A., Hasan, M. A., Ahmed, S., Farooqi, I. H., et al. (2021). Impact, disease outbreak and the eco-hazards associated with pharmaceutical residues: a critical review. *Int. J. Environ. Sci. Technol.* 19, 677–688. doi:10.1007/s13762-021-03158-9
- Krishnan, A., Swarnalal, A., Das, D., Krishnan, M., Saji, V. S., and Shibli, S. M. A. (2024). A review on transition metal oxides based photocatalysts for degradation of synthetic organic pollutants. *J. Environ. Sci.* 139, 389–417. doi:10.1016/j.jes.2023.02.051
- Krobthong, S., Rungsawang, T., Khaodara, N., Kaewtrakulchai, N., Manatura, K., Sukiam, K., et al. (2024). Sustainable development of ZnO nanostructure doping with water hyacinth-derived activated carbon for visible-light photocatalysis. *Toxics* 12 (3), 165. doi:10.3390/toxics12030165
- Kumar, B., Devi, J., Dubey, A., Tufail, A., and Sharma, S. (2024). Exploring the antimalarial, antioxidant, anti-inflammatory activities of newly synthesized transition metal (II) complexes bearing thiosemicarbazone ligands: insights from molecular docking, DFT, MESP and ADMET studies. *Inorg. Chem. Commun.* 159, 111674. doi:10.1016/j.inoche.2023.111674
- Kweiner Tetteh, E., Obotey Ezugbe, E., Asante-Sackey, D., Armah, E. K., and Rathilal, S. (2021). Response surface methodology: photocatalytic degradation kinetics of basic blue 41 dye using activated carbon with TiO₂. *Molecules* 26 (4), 1068. doi:10.3390/molecules26041068
- Lanjwani, M. F., Tuzen, M., Khuhawar, M. Y., and Saleh, T. A. (2024). Trends in photocatalytic degradation of organic dye pollutants using nanoparticles: a review. *Inorg. Chem. Commun.* 159, 111613. doi:10.1016/j.inoche.2023.111613
- Li, K., Gao, S., Wang, Q., Xu, H., Wang, Z., Huang, B., et al. (2015). In-situ-reduced synthesis of Ti³⁺ self-doped TiO₂/g-C₃N₄ heterojunctions with high photocatalytic performance under LED light irradiation. *ACS Appl. Mater. & Interfaces* 7 (17), 9023–9030. doi:10.1021/am508505n
- Lingamdinne, L. P., Koduru, J. R., Choi, Y. L., Chang, Y. Y., and Yang, J. K. (2016). Studies on removal of Pb (II) and Cr (III) using graphene oxide based inverse spinel nickel ferrite nano-composite as sorbent. *Hydrometallurgy* 165, 64–72. doi:10.1016/j.hydromet.2015.11.005
- Liu, J., Shi, H., Sans, C., Sun, L., Yuan, X., Pan, F., et al. (2022). Insights into the photocatalytic ozonation over Ag₂O-ZnO@g-C₃N₄ composite: cooperative structure, degradation performance, and synergistic mechanisms. *J. Environ. Chem. Eng.* 10 (2), 107285. doi:10.1016/j.jece.2022.107285
- Liu, S., Ndago, A. M., Chen, B., Han, S., Chen, W., Zhang, J., et al. (2025). The influence of metal organic frameworks(MOFs) after tannic acid etching on the performance and structure of loose nanofiltration membranes for enhanced dyes/salts selective separation. *J. Water Process Eng.* 70, 107009. doi:10.1016/j.jwpe.2025.107009
- Lopez-Iscosa, P., Pugliese, D., Boetti, N. G., Janner, D., Baldi, G., Petit, L., et al. (2018). Design, synthesis, and structure-property relationships of Er³⁺-doped TiO₂ luminescent particles synthesized by sol-gel. *Nanomaterials* 8 (1), 20. doi:10.3390/nano8010020
- Manogaran, T., Kanagaraj, J., Albeshr, M. F., Selvankumar, T., Palaniappan, M., Arumugam, S., et al. (2024). Enhancing photocatalytic degradation of crystal violet dye with g-C₃N₄/ZnTiO₃ nanocomposites synthesized via a facile approach. *Polym. Adv. Technol.* 35 (4), e6355. doi:10.1002/pat.6355
- Mohamed, A., Mahanna, H., and Samy, M. (2024). Synergistic effects of photocatalysis-periodate activation system for the degradation of emerging pollutants using GO/MgO nanohybrid. *Journal of Environmental Chemical Engineering. Mater. Chem. Phys.* 12(2), 112248. doi:10.1016/j.matchemphys.2023.128401
- Nawaz, R., Arshad, U., Hanafiah, M. M., Haider, S., Anjum, M., Baki, Z. A., et al. (2025). Visible-driven industrial wastewater remediation using black titania: optimization, energy consumption, treatment, and material preparation costs estimation. *Chem. Eng. Sci.* 306, 121257. doi:10.1016/j.ces.2025.121257
- Nawaz, R., Haider, S., Anjum, M., Haneef, T., Oad, V. K., Aqif, M., et al. (2023). Photodegrading hazardous pollutants using black TiO₂ materials with different morphology and estimation of energy requirement. *Mater. Chem. Phys.* 309, 128401. doi:10.1016/j.matchemphys.2023.128401
- Nawaz, R., Hanafiah, M. M., Haider, S., Anjum, M., Ali, M., Khan, R., et al. (2024). Development of energy efficient flower-shaped defective TiO₂ materials for wastewater remediation of agro-industries and oil refineries. *Process Saf. Environ. Prot.* 188, 105–121. doi:10.1016/j.psep.2024.05.058
- Rakkini, A. M., Libu, R. S. R., Vatin, N. I., Devanesan, S., Selvankumar, T., Mary Arul Rosaline, L., et al. (2024). Enhancing photocatalytic activity and biological applications of TiO₂ nanoparticles using Moringa Oleifera leaf extract. *Waste Biomass Valorization* 15, 6523–6537. doi:10.1007/s12649-024-02670-6
- Ramasubramanian, A., Selvaraj, V., Chinnathambi, P., Hussain, S., Ali, D., Kumar, G., et al. (2023). Enhanced photocatalytic degradation of methylene blue from aqueous solution using green synthesized ZnO nanoparticles. *Biomass Convers. Biorefinery* 13 (18), 17271–17282. doi:10.1007/s13399-023-04992-2
- Rani, M., Devi, J., and Kumar, B. (2023). Thiosemicarbazones-based Co (II), Ni (II), Cu (II) and Zn (II) complexes: synthesis, structural elucidation, biological activities and molecular docking. *Chem. Pap.* 77 (10), 6007–6027. doi:10.1007/s11696-023-02917-x

- Ranjitha, S., Bhuvaneshwari, S., Kumar, R. S., Thirumalaisamy, R., Ameer, K., and Selvakumar, T. (2025). Synthesis of nanostructured semiconducting cerium oxide associated titanium dioxide as photoanodic material for dye sensitized solar cells. *Chem. Phys. Impact* 10, 100790. doi:10.1016/j.chphi.2024.100790
- Rao, M., Xia, H., Xu, Y., Jiang, G., Zhang, Q., Yuan, Y., et al. (2024). Study on ultrasonic assisted intensive leaching of germanium from germanium concentrate using HCl/NaOCl. *Hydrometallurgy* 230, 106385. doi:10.1016/j.hydromet.2024.106385
- Rathinavel, T., Ammashi, S., and Marimuthu, S. (2020). Optimization of zinc oxide nanoparticles biosynthesis from *Crateva adansonii* using Box-Behnken design and its antimicrobial activity. *Chem. Data Collect.* 30, 100581. doi:10.1016/j.cdc.2020.100581
- Ruziva, D. T., Oluwalana, A. E., Mupa, M., Meili, L., Selvasembian, R., Nindi, M. M., et al. (2023). Pharmaceuticals in wastewater and their photocatalytic degradation using nano-enabled photocatalysts. *J. Water Process Eng.* 54, 103880. doi:10.1016/j.jwpe.2023.103880
- Selvam, K., Albasher, G., Alamri, O., Sudhakar, C., Selvakumar, T., Vijayalakshmi, S., et al. (2022). Enhanced photocatalytic activity of novel *Canthium coromandelicum* leaves based copper oxide nanoparticles for the degradation of textile dyes. *Environ. Res.* 211, 113046. doi:10.1016/j.envres.2022.113046
- Senasu, T., Chankhanittha, T., Hemavibool, K., and Nanan, S. (2021). Visible-light-responsive photocatalyst based on ZnO/CdS nanocomposite for photodegradation of reactive red dye and ofloxacin antibiotic. *Mater. Sci. Semicond. Process.* 123, 105558. doi:10.1016/j.mssp.2020.105558
- Shukor, S. A. A., Hamzah, R., Bakar, M. A., Noriman, N. Z., Al-Rashdi, A. A., Razlan, Z. M., et al. (2019). Metal oxide and activated carbon as photocatalyst for waste water treatment. *IOP Conf. Ser. Mater. Sci. Eng.* 557 (1), 012066. doi:10.1088/1757-899x/557/1/012066
- Soltani, T., and Lee, B. K. (2016). Mechanism of highly efficient adsorption of 2,4-dinitrophenol by Ag-TiO₂ nanocomposites. *J. Industrial Eng. Chem.* 45, 287–295.
- Srivastava, R. R., Kim, M. S., Lee, J. C., and Ilyas, S. (2015). Liquid-liquid extraction of rhenium (VII) from an acidic chloride solution using Cyanex 923. *Hydrometallurgy* 157, 33–38. doi:10.1016/j.hydromet.2015.07.011
- Subramaniam, S., Kumarasamy, S., Narayanan, M., Ranganathan, M., Rathinavel, T., Chinnathambi, A., et al. (2022). Spectral and structure characterization of *Ferula assafoetida* fabricated silver nanoparticles and evaluation of its cytotoxic and photocatalytic competence. *Environ. Res.* 204, 111987. doi:10.1016/j.envres.2021.111987
- Sultana, K. A., Hernandez Ortega, J., Islam, M. T., Dorado, Z. N., Alvarado-Tenorio, B., Galindo-Esquivel, I. R., et al. (2023). Saccharide-derived zinc oxide nanoparticles with high photocatalytic activity for water decontamination and sanitation. *Sustain. Chem.* 4 (4), 321–338. doi:10.3390/suschem4040023
- Taghizadeh-Lendeh, P., Sarrafi, A. H. M., Alihosseini, A., and Bahri-Laleh, N. (2024). Synthesis and characterisation ZnO/TiO₂ incorporated activated carbon as photocatalyst for gas refinery effluent treatment. *Polyhedron* 247, 116715. doi:10.1016/j.poly.2023.116715
- Thirumoolan, D., Ragupathy, S., Renukadevi, S., Rajkumar, P., Rai, R. S., Kumar, R. S., et al. (2024). Influence of nickel doping and cotton stalk activated carbon loading on structural, optical, and photocatalytic properties of zinc oxide nanoparticles. *J. Photochem. Photobiol. A Chem.* 448, 115300. doi:10.1016/j.jphotochem.2023.115300
- Tian, D., Zhou, H., Zhang, H., Zhou, P., You, J., Yao, G., et al. (2022). Heterogeneous photocatalyst-driven persulfate activation process under visible light irradiation: from basic catalyst design principles to novel enhancement strategies. *Chem. Eng. J.* 428, 131166. doi:10.1016/j.cej.2021.131166
- Wang, X., Xu, G., Tu, Y., Wu, D., Li, A., and Xie, X. (2021). BiOBr/PBCD-BD dual-function catalyst with oxygen vacancies for Acid Orange 7 removal: evaluation of adsorption-photocatalysis performance and synergy mechanism. *Chem. Eng. J.* 411, 128456. doi:10.1016/j.cej.2021.128456
- Wassie, A. T., Ahmed, I. N., Bachheti, A., Husen, A., and Bachheti, R. K. (2024). "Role of zinc oxide nanomaterials for photocatalytic degradation of environmental pollutants," in *Metal and metal-oxide based nanomaterials: synthesis, agricultural, biomedical and environmental interventions* (Singapore: Springer Nature Singapore), 287–311.
- Yang, Y., Guo, Y., Liu, F., Yuan, X., Guo, Y., Zhang, S., et al. (2013). Preparation and enhanced visible-light photocatalytic activity of silver deposited graphitic carbon nitride plasmonic photocatalyst. *Appl. Catal. B Environ.* 142, 828–837. doi:10.1016/j.apcatb.2013.06.026
- Yi, Y., Guan, Q., Wang, W., Jian, S., Li, H., Wu, L., et al. (2023). Recyclable carbon cloth-supported ZnO@Ag₃PO₄ core-shell structure for photocatalytic degradation of organic dye. *Toxics* 11 (1), 70. doi:10.3390/toxics11010070
- Yu, J., Xia, Y., Chen, L., Yan, W., Liu, B., and Jin, S. (2024). Full recovery of brines at normal temperature with process-heat-supplied coupled air-carried evaporating separation (ACES) cycle. *npj Clean. Water* 7, 133. doi:10.1038/s41545-024-00430-6
- Zahedifar, M., and Seyedi, N. (2022). Bare 3D-TiO₂/magnetic biochar dots (3D-TiO₂/BCDs MNPs): highly efficient recyclable photocatalyst for diazinon degradation under sunlight irradiation. *Phys. E Low-dimensional Syst. Nanostructures* 139, 115151. doi:10.1016/j.physe.2022.115151
- Zang, C., Han, X., Chen, H., Zhang, H., Lei, Y., Liu, H., et al. (2022). *In situ* growth of ZnO/Ag₂O heterostructures on PVDF nanofibers as efficient visible-light-driven photocatalysts. *Ceram. Int.* 48 (19), 27379–27387. doi:10.1016/j.ceramint.2022.05.312
- Zhang, X., Li, Y., and Wang, Y. (2018). Photocatalytic degradation of azo dyes using TiO₂-based catalysts: a review. *J. Environ. Chem. Eng.* 6 (2), 2178–2190.